## PAPER

Check for updates

# Synthesis and catalytic activity of palladium supported on heteroatom doped single-wall carbon nanohorns†

Xueyou Tan,[a] Xiaohui Wu,[a] Ziqi Hu,[a] Ding Ma [ID][b] and Zujin Shi [ID] *[a]

The dehydrogenation of indoline to indole is a vital chemical transformation because of the versatile application of indole as an intermediate in the synthesis of medicines or fine chemicals. As a consequence, various approaches are being explored to catalyze dehydrogenation of indoline. Here, we provided a new strategy for dehydrogenation of indoline. Pd nanoparticles supported on boron-, oxygen-, nitrogen- and phosphorus-doped single-wall carbon nanohorns (CNHs) without ligands were synthesized *via* a one-step ultrasonic method. Pd nanoparticles with a diameter of 2–3 nm were dispersed uniformly on heteroatom-doped CNHs. The as-prepared Pd-OCNHs (Pd nanoparticles supported on oxygen-doped CNHs) exhibited excellent performance as the catalyst in dehydrogenation of indoline at a low temperature due to a synergistic effect between metal palladium and oxygen-doped CNHs (OCNHs). In the process, metal palladium offers the main active site for adsorption of indoline, and OCNHs not only act as a carrier, but also provide the active groups (ketonic C=O) for C–H activation of reactants to improve the catalytic activity. Pd-OCNHs could open up a novel way to the dehydrogenation of other heterocycles.

## Introduction

Indole is of great importance for the synthesis of medicines, agrochemicals and fine chemicals as a versatile and significant intermediate.[1] Research into methodologies for indole synthesis is ongoing, and direct dehydrogenation of indoline to indole is the simplest and most effective method among those reported.[2] Dehydrogenation of indoline conventionally needs various oxidizing regents, such as trichlorocyanuric acid,[3] *N-tert*-butylphenylsulfinmidoyl chloride,[4] and manganese dioxide,[5] which are often toxic and harmful, and required in considerable amounts. Researchers have also used Ru-based catalysts (Ru/Al$_2$O$_3$,[6] Ru/Co$_3$O$_4$,[7] Ru(OH)$_X$/Al$_2$O$_3$,[8] *et al.*), Au-based (*e.g.* AuNPs/C[9] and Au/CeO$_2$ (ref. 10)) and Pd-based counterparts (*e.g.* Pd-hydroxyapatite[11] and Pd$_3$Pb/Al$_2$O$_3$ (ref. 12)) for dehydrogenation of indoline and obtained high yields. Although most of these catalysts avoided stoichiometric and environmentally-hazardous oxidants, they need harsh conditions, involving either extra oxidants (*e.g.* O$_2$) or shielding gas (*e.g.* N$_2$) during the reaction process.

Recently, carbon materials (*e.g.* carbon nanotubes (CNTs)[13] and nitrogen-doped graphene (NGr-C)[14] as catalyst support were used for dehydrogenation of indoline. For instance, iron-nitrogen-doped graphene obtained high conversion and yield by using air (15 bar) as a sole oxidant. In this catalytic system, the catalysts synthesis need pyrolysis at high temperature (800 °C) and volume of air required was controlled precisely during catalytic process. In addition, the preparations of carbon materials (CNTs and N-doped graphene) are expensive for mass productions and may introduce metal-impurities due to usage of metal catalysts.[15] The metal-impurities in CNTs are difficult to be removed absolutely, which makes it difficult to identify the nature of proposed synergistic effects. It is noteworthy that single-wall carbon nanohorns (CNHs), an another carbon nanomaterial, could be produced in large scale without using costly metal catalysts by direct current arc discharge method, which makes it cost-effective and metal-free.[16] Herein, we provide a new catalyst support for dehydrogenation reaction of indoline and achieve a high yield only using air, avoiding amount control of air.

CNHs is similar to single-wall carbon nanotubes (CNTs) in structure, but ends up with horn-shaped caps at one end.[17] A single carbon nanohorn has a nanotubular structure with a length between 30–50 nm and diameter ranging from 2–5 nm.[18] CNHs always forms three kinds of aggregates with diameter about 50–100 nm,[19] including dahlida-, bud- and seed-type.[20] Interestingly, heated in oxygen at 693 K or in the presence of nitric acid, CNHs could be oxidized to open the

*[a]Beijing National Laboratory for Molecular Science, State Key Lab of Rare Earth Materials Chemistry and Applications, College of Chemistry and Molecular Engineering, Peking University, Beijing 100871, P. R. China. E-mail: zjshi@pku.edu.cn*
*[b]Beijing National Laboratory for Molecular Science, College of Chemistry and Molecular Engineering, Peking University, Beijing 100871, P. R. China*

nanohorns and create nanowindows on the wall,[21–23] which could prevent the metal nanoparticles (NPs) from sintering and deteriorating,[24] and eventually let NPs enter inside of the CNHs *via* holes on the tube wall.[25] Therefore, CNHs with large surface areas and nanoscale pores is expected to be excellent catalyst support for metal NPs.

Metal supported on CNHs have been widely studied in adsorption,[26] gas storage,[27] drug delivery[28] and catalysts.[29–31] Specially, CNHs often was used for support of palladium nanoparticles (Pd NPs)[22] to prevent from aggregation of Pd NPs and formation of catalytically inactive palladium black.[32] Pd NPs supported on CNHs have been found to be highly efficient in catalysing $H_2$–$O_2$ gas phase reaction, water formation reaction and C–C coupling reactions such as Heck, Suzuki and Stille reaction in the liquid phase.[33–35] However, the preparation methods reported generally required heating at relatively high temperature and ligands such as poly(vinylpyrrolidone) (PVP),[22,24,33] sodium dodecyl sulphate (SDS)[34] and triphenylphosphine (PPh)[36] to connect metal and CNHs, or stabilize and disperse Pd NPs, which could inhibit the catalytic activity.[36]

In this work, we provide a preparation method for Pd NPs supported on heteroatom doped CNHs without the ligands *via* one-step reduction under a mild condition. To our best acknowledge, Pd NPs loaded on the different single-atom doped CNHs, Pd-XCNHs (X, doping atom: B, N, O or P) without ligands have been rarely synthesized and their catalytic properties in dehydrogenation of indoline have not been reported yet. The amazing catalytic activity of Pd-XCNHs for dehydrogenation of indoline could make it suitable to be applied to dehydrogenation of other heterocycles.

## Experiment

### Synthesis of doped CNHs

Pure CNHs was prepared by DC arc-discharge method according to our previous report.[37] BCNHs, NCNHs and PCNHs were produced by DC arc-vaporization of a $B_4C$-containing, melamine-containing and $PPh_3$-containing composite carbon rod in 400 Torr pressure of CO, respectively.[38] The rough carbon materials were roasted at 430 °C for 1 h in the air to remove the amorphous carbon. CNHs was oxidized by a mixture of concentrated acid (the volume ratio of $H_2SO_4$ and $HNO_3$ is 3 : 1) for 3 h to obtain O-doped CNHs (OCNHs).[39]

### Preparation of catalysts

Pd-XCNHs (X = B, N, O or P) were prepared without ligands by one-step reduction method. Briefly, a suspension of 40 mg of carbon support in 8 mL of anhydrous ethanol was prepared by sonicating at room temperature for 30 minutes. Subsequently, 2 mL $K_2PdCl_4$ (9.72 mM) aqueous solution was added into the suspension gradually under ultrasonic conditions, holding for another 2 hours. Then, 1 mL deionized water containing 15 mg $NaBH_4$ was added to this black suspension to reduce Pd precursor to form metal Pd for another 40 minutes. Finally, the black mixture was filtered and washed with deionized water three times. After being dried in a vacuum oven at 80 °C for 8 h,

we obtained Pd nanoparticles supported on carbon materials termed as Pd-CNHs Pd-OCNHs, Pd-NCNHs, Pd-BCNHs and Pd-PCNHs, respectively.

### Characterization

The morphologies of samples were characterized by transmission electron microscopy (TEM) at an accelerating voltage of 200 kV (JEOL-2100). The Pd content in the catalysts were tested by inductively coupled plasma-atomic emission spectrometer (ICP, Prodigy 7). The chemical states of elements and the content in the samples were examined by X-ray photoelectron spectroscopy (XPS, Axis Ultra). Raman measurements were conducted using a 530 nm laser in the back-scattering configuration on a Jobin-Yvon HR800 Spectrometer to obtain the contents of defect in the samples. The Brunauer–Emmett–Teller (BET) method was used to determine the specific surface area by measuring the adsorption of $N_2$ using an ASAP2010 volumetric adsorption analyzer. The X-ray diffraction (XRD) patterns were recorded on a Rigaku MiniFlex 600 using filtered Cu Kα radiation. Fourier transform infrared (FT-IR) spectra of samples in the range of 400–4000 cm$^{-1}$ were investigated with an infrared spectrometric analyzer (Tensor 27, Bruker). Thermogravimetric analysis (TGA) was performed on a Q600 thermogravimetric analyzer (Thermal Analysis Inc., USA) from room temperature to 1000 °C at a rate of 10 °C min$^{-1}$ under an air flow of 100 mL min$^{-1}$.

### Catalytic tests

The dehydrogenation reaction of indoline to indole was carried out in a sealed pressure tube equipped with a reflux condenser. A typical procedure was as follows: 0.06 g (0.5 mmol) indoline, 50 mg catalyst, 5 mL toluene, and 0.06 g dodecane (the internal standard) were placed in a sealed pressure tube. After stirring the heterogeneous mixture at 110 °C or 90 °C for 1 h, the catalyst was removed by filtration. The filtrate was analysed by AgilentGC7820A equipped with a HP-5 column and a FID detector. Each reaction was repeated three times.

## Results and discussion

Fig. 1A showed CNHs and OCNHs exhibited dahlia-type with a diameter of *ca.* 50–100 nm and Pd NPs with a diameter of 2–3 nm were uniformly dispersed on CNHs or OCNHs. However, for doped CNHs with B, N and P atoms, Pd NPs prefer to load on CNHs of bud-type. As shown in Fig. S1 and Table S1,† the specific surface area of Pd-OCNHs (697.4 m$^2$ g$^{-1}$) was larger than Pd-CNHs (672.5 m$^2$ g$^{-1}$), Pd-BCNHs (355.7 m$^2$ g$^{-1}$), Pd-NCNHs (475.4 m$^2$ g$^{-1}$) and Pd-PCNHs (578.9 m$^2$ g$^{-1}$). In addition, the Pd content in the catalysts were shown in Table 1, Pd-OCNHs had the highest content of Pd species (9.99 wt%) among the five catalysts due to its larger specific surface area, which has more nanospaces and nanowindows that are in favour of the tailoring of Pd NPs.

Furthermore, XRD diffraction patterns of samples in the samples were shown in Fig. 2. All samples exhibited the diffraction characteristic peaks of carbon as well as Pd
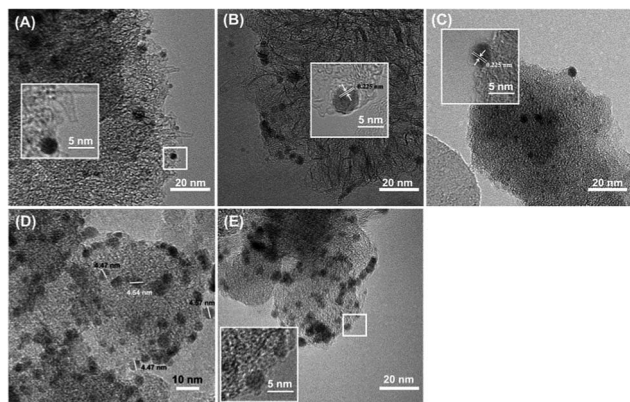
Fig. 1 TEM images of (A) Pd-CNHs, (B) Pd-OCNHs, (C) Pd-BCNHs, (D) Pd-NCNHs, and (E) Pd-PCNHs, respectively, insets show Pd NPs at a high magnification.



Fig. 2 XRD diffraction patterns of samples.

diffraction peaks. The diffraction peaks at 26.35, 42.77 and 54.66° are correspondent with the (002), (100) and (004) facet of CNHs,[40] respectively. The new peaks at 40.00, 46.63 and 68.19° in Pd-XCNHs are respectively ascribed to the (111), (200) and (220) facet of Pd face-centered cubic (FCC) structure.[41,42] The lattice $d$-spacing of (111) plane calculated is approximately 0.225 nm according to Bragg's law,[43] which is confirmed by HRTEM in Fig. 1B and C. The peak representing Pd (111) was recognized clearly so that it was used to estimate the crystalline size. According to Debye–Scherrer method, the relationship between the average size of particles and the full width at a half max (FWHW) of diffraction peak is inversely proportional.[44] Pd-NCNHs had the smallest FWHW among the samples, and hence the largest size of Pd NPs. This result was consistent well with the result of TEM, where the Pd NPs with a diameter of 4–5 nm were uniformly loaded on NCNHs (Fig. 1D).

Subsequently, the chemically structural features of samples were investigated by FT-IR spectroscopy. The characteristic peaks of Pd-XCNHs in Fig. 3A were nearly the same, which implied that Pd-XCNHs had the similar framework structures and functional groups. The band at 1720 cm$^{-1}$ was assigned to ketonic C=O groups in the samples.[45,46] It has been reported that ketonic C=O is considered to be an active site of C–H by coordinating with C–H bond,[47] which could improve the catalytic activity of the reactions involving activation of C–H bonds. Moreover, the Raman spectroscopy was used to study the surface defects of the sample. As shown in Fig. 2B, the G band at approximately 1590 cm$^{-1}$ and the D band at near 1350 cm$^{-1}$ are the graphitic carbon peaks and the disordered carbon peaks,[48,49] respectively. The higher $I_D/I_G$ ratio in doping CNHs implies the more defect and disordered carbon of sample.[50–52] Pd-BCNHs
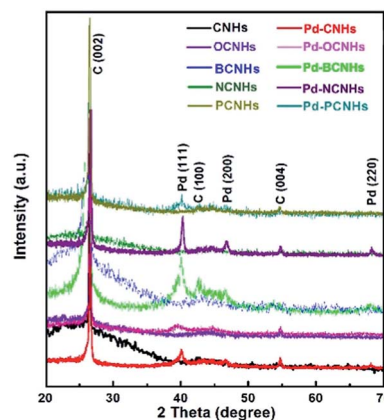
($I_D/I_G = 1.17$), Pd-NCNHs ($I_D/I_G = 1.20$), Pd-OCNHs ($I_D/I_G = 1.47$) and Pd-PCNHs ($I_D/I_G = 1.32$) had more defective carbon compared with Pd-CNHs ($I_D/I_G = 1.06$). Indeed, Pd-OCNHs, Pd-NCNHs and Pd-PCNHs also showed the obvious peaks originating from X-doped defective carbon at 439, 467 and 532 °C in DTG curves (see Fig. S2†),[38] respectively. Raman and TGA characterizations indicated that heteroatom doped CNHs had more defective carbon compared with pure CNHs, which could affect the reaction activity.[47]

The surface state and chemical composition of samples were studied by X-ray photoelectron spectroscopy (XPS). The relative surface concentrations of the individual elements are shown in Table S2.† The XPS spectra of Pd 3d of five catalysts are shown in Fig. 4A. Pd $3d^{5/2}$ (335.8 eV), Pd $3d^{3/2}$ (341.1 eV) and Pd $3d^{5/2}$ (337.2 eV), Pd $3d^{3/2}$ (342.4 eV) were assigned to Pd$^0$ and Pd$^{2+}$,[53,54] respectively. The presence of characteristic peaks of Pd 3d in Fig. 4A unambiguously demonstrated that Pd NPs had been successfully loaded on CNHs. In the Table S3,† Pd-OCNHs (61.73%) and Pd-BCNHs (60.88%) contained more Pd$^0$ than Pd-CNHs (32.95%), Pd-NCNHs (32.54%) and Pd-PCNHs (33.51%) in the surface of samples. Some previous studies have been reported that Pd$^0$ plays a vital role in dehydrogenation of indoline.[11,12] In the B 1s spectra, the peaks at 186.7, 188.3 and 193.3 eV can be respectively ascribed to B–C$_4$, B–C$_3$ and B–O,[38,55] and the peak at 188.3 eV indicated that the B element enters the graphite sheet lattice. Two kinds of N species including pyridinic N (398.7 eV) and pyrrolic N (400.2 eV)[56] were found in the Pd-NCNHs in Fig. 4D. The peak at 133.4 eV and 135.5 eV in the Fig. 4E could be derived respectively from P–C and P–O of Pd-PCNHs.[38,55] These results indicated the boron, nitrogen atom, and phosphorus atoms had been doped into the corresponding materials carbon materials successfully. As we can see, Fig. 4B showed four peaks corresponding to oxygen atoms of carboxyl (534.3–535.4 eV), ether oxygen atoms in esters and anhydrides (533.1–533.8 eV), C=O in esters, amides, anhydrides and O atoms in hydroxyl or ethers (532.3–532.8 eV), and ketonic C=O groups (531.0–531.5 eV).[56,57] Oxygen-containing functional groups in Pd-CNHs, Pd-BCNHs, Pd-NCNHs and Pd-PCNHs were mainly derived from CO during the carbon nanomaterials synthesis. Pd-OCNHs had the highest

Table 1 The Pd content in the catalysts were determined by ICP

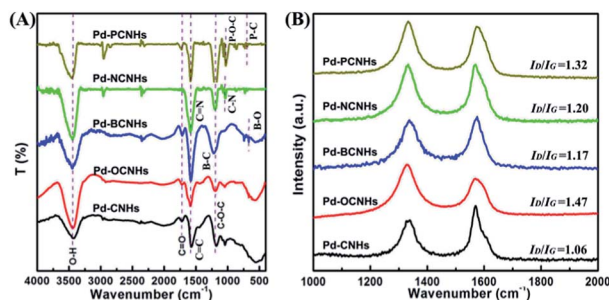| Sample | Pd-CNHs | Pd-OCNHs | Pd-BCNHs | Pd-NCNHs | Pd-PCNHs |
| --- | --- | --- | --- | --- | --- |
| Pd content (wt%) | 4.69 | 9.99 | 5.61 | 5.63 | 5.63 |

**Fig. 3** (A) FT-IR spectra of the samples; (B) Raman spectra of the catalysts, the $I_D/I_G$ represent the intensity ratio of D band and G band of catalysts, respectively.

content of ketonic C=O groups (about 25%) in the surface due to mixed acid oxidation.

Finally, we investigated the catalytic capabilities of Pd catalysts for dehydrogenation of indoline at 110 °C. As shown in Table 2, Pd-XCNHs all exhibited high catalytic activities (conversion rate: 100%; yield: >99%) without adding any oxidants, which were being widely used in the previously reported catalysts (e.g. Ru/Co$_3$O$_4$,[7] AuNPs/C,[9] and Pd$_3$Pb/Al$_2$O$_3$ (ref. 12)) under the same temperature (110 °C), while other catalysts (e.g. AuNPs/C, Ru/Co$_3$O$_4$ and Cu/Al$_2$O$_3$ (ref. 58)) were reported involving either O$_2$ or shielding gas (e.g. N$_2$ and Ar). To further explore the role of the catalysts in the mechanism, catalytic activities of Pd NPs supported on the different heteroatoms-doped CNHs, Pd-BCNHs, Pd-NCNHs Pd-OCNHs and Pd-PCNHs, were investigated at low temperature of 90 °C. As shown in Table 3, Pd-OCNHs (61.73% Pd$^0$) showed the highest catalytic activity at 90 °C among the above catalysts and obtained a high conversion rate (100%) and yield (93%), while

**Table 2** The dehydrogenation of indoline to indole using the various catalysts at 110 °C[a]

| Entry | Catalyst | Conv. (%) | Yield (%) |
|---|---|---|---|
| 1 | None | 19 | 9 |
| 2 | K$_2$PdCl$_4$ | 100 | 45 |
| 3 | CNHs | 32 | 22 |
| 4 | OCNHs | 44 | 22 |
| 5 | BCNHs | 46 | 30 |
| 6 | NCNHs | 32 | 21 |
| 7 | PCNHs | 32 | 18 |
| 8 | Pd-CNHs | 100 | >99 |
| 9 | Pd-OCNHs | 100 | >99 |
| 10 | Pd-BCNHs | 100 | >99 |
| 11 | Pd-NCNHs | 100 | >99 |
| 12 | Pd-PCNHs | 100 | >99 |

[a] Reaction conditions: substrate, 0.5 mmol; catalyst, 50 mg; solvent, 5 mL (toluene); temperature, 110 °C; time, 1 h.

Pd-BCNHs (60.88% Pd$^0$), Pd-CNHs (32.95% Pd$^0$), Pd-NCNHs (32.54% Pd$^0$), Pd-PCNHs (33.51% Pd$^0$) and K$_2$PdCl$_4$ (0% Pd$^0$) obtained 66, 54, 45, 17 and 9% yield, respectively. These results indicated that Pd$^0$ species play a crucial role during the dehydrogenation process.

Based on the above results and previously researches,[7,9,12] we speculated a possible catalytic mechanism for the composites in dehydrogenation of indoline in Scheme 1. Firstly, the N atom of indoline coordinated to the Pd$^0$.[59] Then, C–H bond adjacent to the N atom was activated.[11] Subsequently, the intermediate
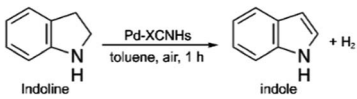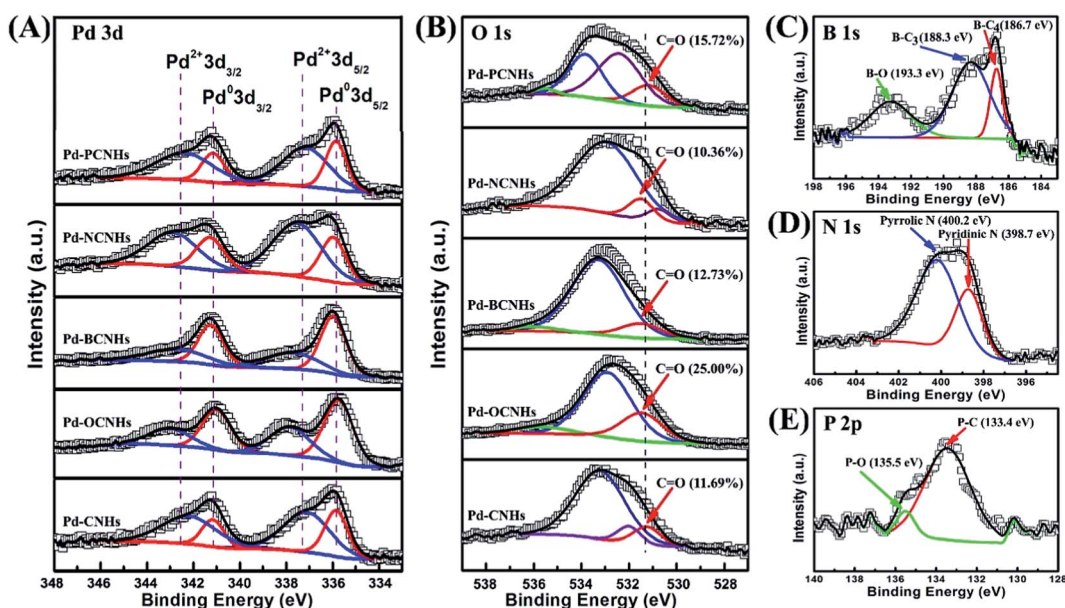


**Fig. 4** (A) Pd 3d XPS spectra of catalysts; (B) O 1s XPS spectra of catalysts; (C) B 1s XPS spectra of Pd–BCNHs; (D) N 1s XPS spectra of Pd–NCNHs; (E) P 2p XPS spectra of Pd–PCNHs.

**Table 3** The dehydrogenation of indoline to indole using the various catalysts at 90 °C[a]



| Entry | Catalyst | Conv. (%) | Yield (%) |
|-------|----------|-----------|-----------|
| 1 | None | 17 | 8 |
| 2 | $K_2PdCl_4$ | 15 | 9 |
| 3 | CNHs | 28 | 19 |
| 4 | OCNHs | 39 | 24 |
| 5 | BCNHs | 33 | 20 |
| 6 | NCNHs | 29 | 18 |
| 7 | PCNHs | 21 | 15 |
| 8 | Pd-CNHs | 71 | 54 |
| 9 | Pd-OCNHs | 100 | 93 |
| 10 | Pd-BCNHs | 81 | 66 |
| 11 | Pd-NCNHs | 56 | 45 |
| 12 | Pd-PCNHs | 25 | 17 |

[a] Reaction conditions: substrate, 0.5 mmol; catalyst, 50 mg; solvent, 5 mL (toluene); temperature, 90 °C; time, 1 h.

species underwent β-hydride elimination to form indole.[9] Finally, hydrogen species was removed by oxygen.[12] Although the interaction between the aromatic ring of indoline and the π electron of the CNHs may be weak, it could not be ignored because the π···π interaction favours the adsorption of indoline in planar fashion. The similar argument has been reported in the study for Pd@carbon nitride catalysing hydrogenation of phenol.[60]

It is noteworthy that metal-free CNHs (BCNHs, NCNHs, OCNHs and PCNHs) also had catalytic activities (in Table 2), and the yield increased with increasing ketonic C=O content from 18% (NCNHs, 10.36% C=O) through 19% (CNHs, 11.69% C=O) and 20% (BCNHs, 12.73% C=O) to 24% (OCNHs, 25.00% C=O). Nevertheless, PCNHs (15.72% C=O) only achieved a yield of 15%. Combining with results of Raman, XPS and TGA characterizations, we speculate two reasons to clarify this contradiction. On one hand, PCNHs holds more surface defects by the introduction of P atoms than BCNHs and NCNHs do, which reduces the flatness of CNHs and weakens the π···π interaction between CNHs and indoline, leading to the



**Scheme 1** The proposed reaction mechanism of Pd supported on doped CNHs.

inhibited activity of PCNHs. In this regard, although Pd-CNHs, Pd-NCNHs and Pd-PCNHs had nearly equivalent proportion of Pd[0], Pd-PCNHs ($I_D/I_G = 1.32$) with more defective carbon exhibited lower activity for dehydrogenation of indoline. On the other hand, the surface of OCNHs has rich ketonic C=O, a nucleophilic species, which preferentially reacts with electron-deficient saturated bonds and promotes the activation of C–H[47] adjacent to the nitrogen atom, resulting in higher activity than those of other metal-free CNHs. Thus, although Pd-OCNHs and Pd-BCNHs had the approximate content of Pd[0], Pd-OCNHs containing lots of ketonic C=O showed higher activity than Pd-BCNHs does. Based on the above discussion, we believe that Pd[0] is the main active site for adsorption of indoline during the catalytic process, and ketonic C=O of OCNHs is the active groups for C–H bond activation. Therefore, the excellent catalytic activity of Pd-OCNHs in dehydrogenation of indoline is the result of synergistic action between metal palladium and OCNHs.

It is noteworthy that although CNTs is similar to CNHs in structure, CNTs produced by chemical vapor deposition (CVD) or other methods may contain some ineradicable metal-impurities (such as Ni[61] or Fe[61,62], et al.), resulting in more complicated reaction mechanism. Indeed, iron oxide component has been reported to catalyse dehydrogenating of indoline.[14] Thus, metal impurity-free Pd-OCNHs here is a more suitable paradigm to investigate the catalytic mechanism for dehydrogenation of indoline.

## Conclusions

In summary, we have successfully synthesized Pd NPs with diameter of 2–3 nm dispersed uniformly on B-, N-, O-, P-doped CNHs without ligands via one-step reduction method. Pd-OCNHs contained high content of palladium species due to large BET specific surface area and exhibited the highest catalytic activity among all the catalysts in the dehydrogenating of indoline to indole. These results indicate that the remarkable activity of Pd-OCNHs originates in synergistic effect between metal palladium and OCNHs. Metal palladium is the main active site for adsorption of indoline during the catalytic process, OCNHs with lots of ketonic C=O not only acts as a carrier, but also provides the active groups (ketonic C=O) for C–H bond activation of reactant to improve the catalytic activity. We believe that the Pd-OCNHs here can also be applied to dehydrogenation of other heterocycles as catalyst with outstanding catalytic activity.

## Acknowledgements

## Notes and references

1 R. J. Sundberg, *The chemistry of indoles*, Academic Press, New York, 1970.
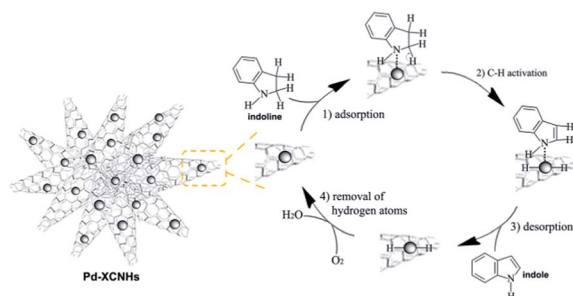
2   M. N. Preobrazhenskaya, *Russ. Chem. Rev.*, 1967, **36**, 753.

3   U. Tilstam, M. Harre, T. Heckrodt and H. Weinmann, *Tetrahedron Lett.*, 2001, **42**, 5385.

4   T. Mukaiyama, A. Kawana, Y. Fukuda and J. Matsuo, *Chem. Lett.*, 2001, 390.

5   A. B. A. Jansen, J. M. Johnson and J. R. J. Surtees, *J. Chem. Soc.*, 1964, 5573.

6   K. Yamaguchi and N. Mizuno, *Angew. Chem., Int. Ed.*, 2003, **42**, 1480.

7   F. Li, J. Chen, Q. Zhang and Y. Wang, *Green Chem.*, 2008, **10**, 553.

8   K. Kamata, J. Kasai, K. Yamaguchi and N. Mizuno, *Org. Lett.*, 2004, **6**, 3577.

9   M.-H. So, Y. Liu, C.-M. Ho and C.-M. Che, *Chem.–Asian J.*, 2009, **4**, 1551.

10  L. Aschwanden, T. Mallat, F. Krumeich and A. Baiker, *J. Mol. Catal. A: Chem.*, 2009, **309**, 57.

11  T. Hara, K. Mori, T. Mizugaki, K. Ebitani and K. Kaneda, *Tetrahedron Lett.*, 2003, **44**, 6207.

12  S. Furukawa, A. Suga and T. Komatsu, *Chem. Commun.*, 2014, **50**, 3277.

13  D. V. Jawale, E. Gravel, N. Shah, V. Dauvois, H. Li, I. N. N. Namboothiri and E. Doris, *Chem.–Eur. J.*, 2015, **21**, 7039.

14  X. Cui, Y. Li, S. Bachmann, M. Scalone, A.-E. Surkus, K. Junge, C. Topf and M. Beller, *J. Am. Chem. Soc.*, 2015, **137**, 10652.

15  P. Nikolaev, M. J. Bronikowski, R. K. Bradley, F. Rohmund, D. T. Colbert, K. A. Smith and R. E. Smalley, *Chem. Phys. Lett.*, 1999, **313**, 91.

16  Y. Tao, D. Noguchi, C.-M. Yang, H. Kanoh, H. Tanaka, M. Yudasaka, S. Iijima and K. Kaneko, *Langmuir*, 2007, **23**, 9155.

17  S. Ustsumi, K. Urita, H. Kanoh, M. Yudasaka, K. Suenaga, S. Iijima and K. Kaneko, *J. Phys. Chem. B*, 2006, **110**, 7165.

18  V. Krungleviciute, A. D. Migone and M. Pepka, *Carbon*, 2009, **47**, 769.

19  R. Yuge, T. Ichihashi, Y. Shimakawa, Y. Kubo, M. Yudasaka and S. Iijima, *Adv. Mater.*, 2004, **16**, 1420.

20  T. Azami, D. Kasuya, R. Yuge, M. Yudasaka, S. Iijima, T. Yoshitake and Y. Kubo, *J. Phys. Chem. C*, 2008, **112**, 1330.

21  S. Utsumi, J. Miyawaki, H. Tanaka, Y. Hattori, T. Itoi, N. Ichikuni, H. Kanoh, M. Yudasaka, S. Iijima and K. Kaneko, *J. Phys. Chem. B*, 2005, **109**, 14319.

22  E. Bekyarova, A. Hashimoto, M. Yudasaka, Y. Hattori, K. Murata, H. Kanoh, D. Kasuya, S. Iijima and K. Kaneko, *J. Phys. Chem. B*, 2005, **109**, 3711.

23  R. Yuge, T. Ichihashi, Y. Shimakawa, Y. kubo, M. Yudasaka and S. Iijima, *Adv. Mater.*, 2004, **16**, 1420.

24  T. Itoh, K. Urita, E. Bekyarova, M. Arai, M. Yudasaka, S. Iijima, T. Ohba, K. Kaneko and H. Kanoh, *J. Colloid Interface Sci.*, 2008, **322**, 209.

25  R. Yuge, T. Ichihashi, J. Miyawaki, T. Yoshitake, S. Iijima and M. Yudasaka, *J. Phys. Chem. C*, 2009, **113**, 2741.

26  J. Fan, M. Yudasaka, Y. Kasuya, D. Kasuya and S. Iijima, *Chem. Phys. Lett.*, 2004, **397**, 5.

27  N. Sano, K. Taniguchi and H. Tamon, *J. Phys. Chem. C*, 2014, **118**, 3402.

28  K. Ajima, A. Maigne, M. Yudasaka and S. Iijima, *J. Phys. Chem. B*, 2006, **110**, 19097.

29  M. Kosaka, S. Kuroshima, K. Kobayashi, S. Sekino, T. Ichihashi, S. Nakamura, T. Yoshitake and Y. Kubo, *J. Phys. Chem. C*, 2009, **113**, 8660.

30  K. Murata, M. Yudasaka and S. Iijima, *Carbon*, 2006, **44**, 799.

31  T. Koshitake, Y. Shimakawa, S. Kuroshima, H. Kimura, T. Ichihashi, Y. Kubo, D. Kasuya, K. Takahashi, F. Kokai, M. Yudasaka and S. Iijima, *Phys. B*, 2002, **323**, 124.

32  A. H. M. de Vries, J. M. C. A. Mulders, J. H. M. Mommers, H. J. W. Henderickx and J. G. de Vries, *Org. Lett.*, 2003, **5**, 3285.

33  S. Zhu and G. Xu, *Nanoscale*, 2010, **2**, 2538.

34  N. Karousis, T. Ichihashi, M. Yudasaka, S. Iijima and N. Tagmatarchis, *J. Nanosci. Nanotechnol.*, 2009, **9**, 6047.

35  T. Itoh, H. Danjo, W. Sasaki, K. Urita, E. Bekyarova, M. Arai, T. Imamoto, M. Yudasaka, S. Iijima, H. Kanoh and K. Kaneko, *Carbon*, 2008, **46**, 172.

36  J. G. de Vries, *Dalton Trans.*, 2006, 421.

37  N. Li, Z. Wang, K. Zhao, Z. Shi, Z. Gu and S. Xu, *Carbon*, 2010, **48**, 1580.

38  X. Wu, L. Cui, P. Tang, Z. Hu, D. Ma and Z. Shi, *Chem. Commun.*, 2016, **52**, 5391.

39  L. Cui, Y. Liu, X. Wu, Z. Hu, Z. Shi and H. Li, *RSC Adv.*, 2015, **5**, 75817.

40  T. A. Saleh, *Appl. Surf. Sci.*, 2011, **257**, 7746.

41  Y. Yan, X. Jia and Y. Yang, *Catal. Today*, 2016, **259**, 292.

42  C. Poonjarernsilp, N. Sano, T. Charinpanitkul, H. Mori, T. Kikuchi and H. Tamon, *Carbon*, 2011, **49**, 4920.

43  F. Wolfers, *C. R. Hebd. Seances Acad. Sci.*, 1923, **177**, 759.

44  B. D. Hall, D. Zanchet and D. Ugarte, *J. Appl. Crystallogr.*, 2000, 1335.

45  N. Kizilcan and B. Erson, *Pigm. Resin Technol.*, 2015, **44**, 198.

46  J. Y. Kim, S. Morisada, H. Kawakita, K. Ohto and Y. Kim, *J. Inclusion Phenom. Macrocyclic Chem.*, 2015, **82**, 25.

47  J. Zhang, X. Liu, R. Blume, A. Zhang, R. Schlögl and D. S. Su, *Science*, 2008, **322**, 73.

48  A. Malesevic, R. Vitchev, K. Schouteden, A. Volodin, L. Zhang, G. V. Tendeloo, A. Vanhulsel and C. V. Haesendonck, *Nanotechnology*, 2008, **19**, 305604.

49  F. Parvizi, D. Teweldebrhan, S. Ghosh, I. Calizo, A. A. Balandin, H. Zhu and R. Abbaschian, *Micro Nano Lett.*, 2008, **3**, 29.

50  D. Y. Kim, C.-M. Yang, H. Noguchi, M. Yamamoto, T. Ohba, H. Kanoh and K. Kaneko, *Carbon*, 2008, **46**, 611.

51  Z.-H. Sheng, H.-L. Gao, W.-J. Bao, F.-B. Wang and X.-H. Xia, *J. Mater. Chem.*, 2012, **22**, 390.

52  C.-W. Tsai, M.-H. Tu, C.-J. Chen, T.-F. Hung, R.-S. Liu, W.-R. Liu, M.-Y. Lo, Y.-M. Peng, L. Zhang, J. Zhang, D.-S. Shy and X.-K. Xing, *RSC Adv.*, 2011, **1**, 1349.

53  H. Jin, T. Xiong, Y. Li, X. Xu, M. Li and Y. Wang, *Chem. Commun.*, 2014, **50**, 12637.

54  X. Xu, Y. Li, Y. Gong, P. Zhang, H. Li and Y. Wang, *J. Am. Chem. Soc.*, 2012, **134**, 16987.

55 P. Tang, G. Hu, Y. Gao, W. Li, S. Yao, Z. Liu and D. Ma, *Sci. Rep.*, 2014, **4**, 1.

56 L. Sun, C. Wang, Y. Zhou, X. Zhang, B. Cai and J. Qiu, *Appl. Surf. Sci.*, 2013, **277**, 88.

57 J.-H. Zhou, Z.-J. Sui, J. Zhu, P. Li, D. Chen, Y.-C. Dai and W.-K. Yuan, *Carbon*, 2007, **45**, 785.

58 D. Damodara, R. Arundhathi and P. R. Likhar, *Adv. Synth. Catal.*, 2014, **356**, 189.

59 S.-I. Murahashi, N. Yoshimura, T. Tsumiyama and T. Kojima, *J. Am. Chem. Soc.*, 1983, **105**, 5002.

60 Y. Wang, J. Yao, H. Li, D. Su and M. Antonietti, *J. Am. Chem. Soc.*, 2011, **133**, 2362.

61 D. Yuan, L. Ding, H. Chu, Y. Feng, T. P. McNicholas and J. Liu, *Nano Lett.*, 2008, **8**, 2576.

62 P. Nikolaev, M. J. Bronikowski, R. K. Bradley, F. Rohmund, D. T. Colbert, K. A. Smith and R. E. Smalley, *Chem. Phys. Lett.*, 1999, **313**, 91.